PAPER

Check for updates

Discriminative light-up detection of volatile chlorinated solvents and dual-phase encrypted security ink†

Retwik Parui,[a] Niranjan Meher [ID] [ab] and Parameswar Krishnan Iyer [ID] *[ac]

The highly toxic nature of volatile chlorinated solvents (VCSs) demands precise detection and discrimination techniques to check the quality of air and groundwater. However, the analogous structural behaviour of these VCSs makes this highly challenging. Herein, a "light-up" colorimetric and fluorometric strategy has been developed for the discriminative detection of volatile chlorinated solvents (VCSs) on multiple platforms. Three luminophores have been strategically designed and synthesized through a simple, efficient and catalyst-free procedure. Upon UV irradiation, the designed naphthalene-based fluorophores can distinctly detect specific VCSs *via* photoinduced ground-state complexation, which leads to the discriminative recognition of chloroform in both the liquid and vapor phases and provides a portable, cost-effective platform for on-site application. In particular, the solid-state non-fluorescence property of one of the naphthalene congeners (NCPh) has been successfully translated into a robust dual-phase encrypted security ink for data protection.

Introduction

Volatile chlorinated solvents (VCSs) are extensively used in industrial applications and research laboratories, which make them highly likely to cause severe contamination and workplace explosions.[1–4] Excessive exposure to VCSs is critically threatening to health in terms of eye irritation, heart disease, severe headache, kidney failure, and respiratory dysfunction that can even lead to death.[5–8] Thus, highly sensitive as well as selective sensing systems for VCSs are in huge demand to efficiently counter their hazardous nature. Luminescent materials are excellent alternatives to conventional analytical techniques[9–11] such as GC-MS and infrared spectrometry due to their easy handling procedures and high selectivity towards target analytes.[12,13] To date, a wide range of fluorescent sensors[14–18] have been developed based on the concept of solvatochromism, but the spectral overlaps make it extremely difficult to discriminate the frequently used VCSs.[19,20] To the

best of our knowledge, very few materials have been developed with remarkable sensitivity for the detection of trace quantities of VCSs along with discriminative ability.[21,22] Hence, the development of "light-up" sensing systems for the precise discriminative detection of VCSs with the ability for on-site application is far from trivial.

Herein, three naphthalene-based probes, NBPh, NCPh, and NBMe, have been synthesized, which demonstrate swift light-up colorimetric and fluorometric responses towards chloroform in the presence of UV light in both solution and vapor phases. Despite having very similar structural and electronic properties, these probes efficiently discriminate four common VCSs: chloroform, carbon tetrachloride, 1,2-dichloromethane and chlorobenzene.

Most importantly, the unique chemistry of these naphthalene-based probes with chloroform in the presence UV light has been strategically utilized to develop a robust dual-phase encrypted security ink for data encryption (Fig. 1(a)).
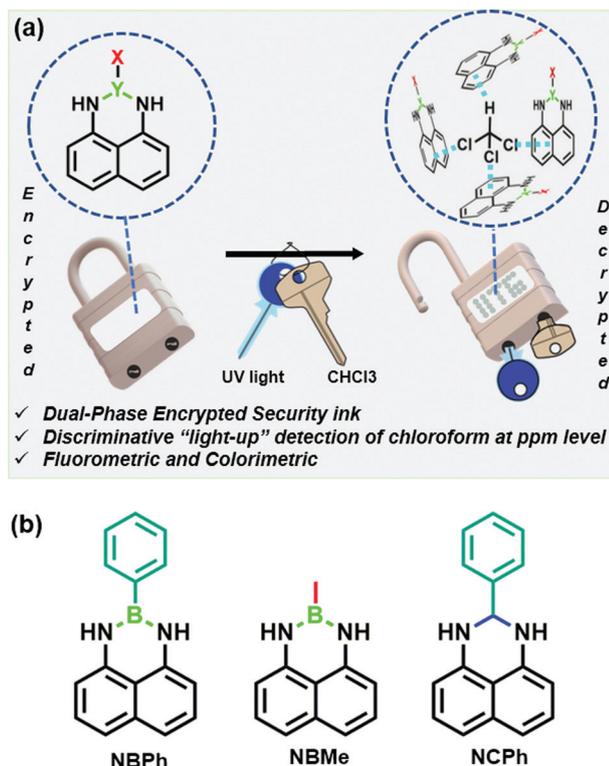
[a] *Department of Chemistry, Indian Institute of Technology Guwahati, Guwahati 781039, India. E-mail: pki@iitg.ac.in*

[b] *Currently at Department of Radiology and Biomedical Imaging, University of California San Francisco, CA 94107, USA*

[c] *Centre for Nanotechnology, Indian Institute of Technology Guwahati, Guwahati 781039, India*

† Electronic supplementary information (ESI) available: Experimental details, characterization spectra (^{1}H and ^{13}C NMR, HRMS), comparison table, theoretical data, TRPL data, NMR, FTIR titration data and additional figures, Fig. S1–S17, Movie SV-1–6. See DOI: https://doi.org/10.1039/d2ma00319h

Results and discussion

Considering the exceptional luminescence characteristics of boron-incorporated molecules, the naphthalene-based fluorescent probes were strategically synthesized through a simple, efficient and catalyst-free procedure for the light-up detection of VCSs (Fig. 1(b)).[23] The three congeners 2-methyl-2,3-dihydro-1*H*-naphtho[1,8-*de*][1,3,2]diazaborinine (NBMe), 2-phenyl-2,3-dihydro-1*H*-naphtho[1,8-*de*][1,3,2]diazaborinine (NBPh) and

Fig. 1 (a) Graphical representation of the working principle of the dual-phase encrypted security ink-based light-up decryption. (b) Chemical structures of NBMe, NBPh and NCPh molecules highlighting the specific differences in their functionalities.

2-phenyl-2,3-dihydro-1*H*-perimidine (NCPh) were systematically evaluated to obtain a clear insight of the sensing mechanism. 1,8-Diaminonaphthalene was used as a synthetic precursor to obtain all the congeners. The synthesis of the six-membered diazaborinines (NBMe, NBPh) involves dehydration of a diamine and boronic acid, with concurrent ring formation. NCPh was obtained through the condensation reaction between a diamine and benzaldehyde. The phenyl ring and boron atom of the NBPh molecule were strategically replaced by a methyl group in NBMe and a carbon atom in NCPh to precisely compare and understand the interaction and sensing ability of the probes with chloroform (Scheme S1, ESI†). The characterization studies *via* HRMS and NMR (^{1}H, ^{13}C), of all the three probes are presented in the ESI.†

UV/visible and fluorescence studies were conducted for all three probes (20 μM) in chloroform (Fig. 2). The PL spectrum of NBPh showed a broad spectrum with very low fluorescence intensity (Fig. 2(a)). However, this intensity (λ_{max} = 470 nm) increased gradually following back-to-back recording of the fluorescence emission spectra (each taking ∼45 s) in the wavelength window of 340–650 nm (λ_{ex} = 330 nm). Fluorescence intensity was amplified 12-fold within 15 min of irradiation, as confirmed by the fluorescence kinetics study (Fig. 2(a), inset a1). The UV/visible spectrum of the corresponding solution recorded before and after obtaining the emission spectra

(Fig. 2(d)) showed strong new absorption bands at 760 nm and 435 nm with a significant decrease in the absorption peak at 330 nm. This clearly indicated the formation of ground-state complexation between the probe and the chloroform molecule, with a visual light-up green color of the solution, which aligns with the new absorption band in the red region, and the long wavelength band could be ascribed as the charge transfer (CT) band.[24] Besides, such complexation behavior also suggests the prominent role of irradiated UV light, confirmed by further recording the UV/visible and fluorescence spectra of the probes with and without irradiation of UV light (365 nm) after 15 minutes (Fig. S1, ESI†). Similar studies performed with the NBMe and NCPh probes demonstrated comparable behavior in their fluorescence (Fig. 2(b) and (c)) and absorption spectra (Fig. 2(e) and (f)). The fluorescence quantum yields (QY) of NBPh, NCPh and NBMe in chloroform were calculated using quinine sulfate as a reference and their QY increased drastically from 0.005, 0.003 and 0.007 to 0.164, 0.057 and 0.285, respectively, after 15 minutes of UV exposure. These results clearly demonstrate the key role of UV light in the complexation reaction of these probes with chloroform, which leads to a strong colorimetric and fluorometric response and subsequently to the development of a dual-phase encrypted security ink.

To evaluate the practical utility of these probes, their sensitivity and selectivity towards chloroform were analyzed carefully. The fluorescence emission of the NBMe probe, evaluated in the presence of common organic solvents, showed a distinctive light-up green emission only in the presence of chloroform (Fig. 3(a), (b) and Movie SV-1, ESI†). Selectivity studies of NBPh and NCPh towards various solvents also indicated the high selectivity of these probes towards chloroform (Fig. S2 and Movie SV-2, 3, ESI†). To explore their sensitivity, different percentages of chloroform were added to 20 μM NBMe in methanol, and the fluorescence emission kinetics were recorded following one hour exposure to UV light at 330 nm. On gradually increasing the chloroform percentage in methanol, the fluorescence intensity also grew steadily. By using the standard equation[25] ($n\sigma/K$, where n = 3, σ = standard deviation, K = slope of the equation), the limit of detection (LOD) for chloroform was calculated to be 7.95 ppm, which is one of the best values reported to date (Fig. 3(c), (d) and Table S1, ESI†). Both NBPh and NCPh were also found to be highly sensitive towards chloroform with LOD values of 168.5 ppm and 74.9 ppm, respectively (Fig. S3, ESI†). However, among the three probes, the NBMe molecule displayed excellent selectivity and sensitivity towards chloroform. Apart from the selective light-up detection of chloroform, the NBMe probe could also efficiently discriminate structurally similar VCSs. The NBMe probe showed a strong fluorescence light-up emission at 470 nm in the presence of CHCl$_3$, which turns into an intense blue-green emission under UV irradiation for 15 min (Fig. 4(a)). On the contrary, NBMe remained in a nearly quenched state in carbon tetrachloride (CCl$_4$) (Fig. 4(b)), while an intense deep blue emission was observed in both 1,2-dichloromethane (CH$_2$Cl$_2$) and chlorobenzene (PhCl), where a steady reduction
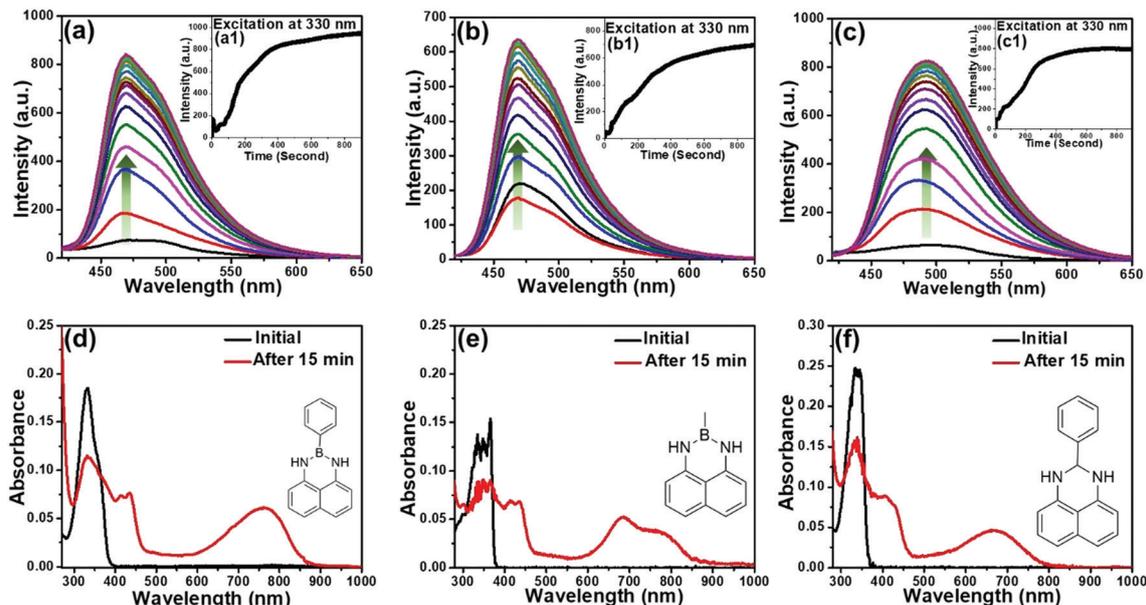
Fig. 2 Fluorescence spectra of (a) NBPh, (b) NBMe and (c) NCPh in chloroform (20 μM, λ_{ex} = 330 nm) with back-to-back reading. Insets: (a1), (b1), and (c1) are the corresponding fluorescence kinetic graphs at λ_{max} with respect to time (λ_{ex} = 330 nm). UV/visible spectra of (d) NBPh, (e) NBMe and (f) NCPh before and after UV irradiation at 330 nm.
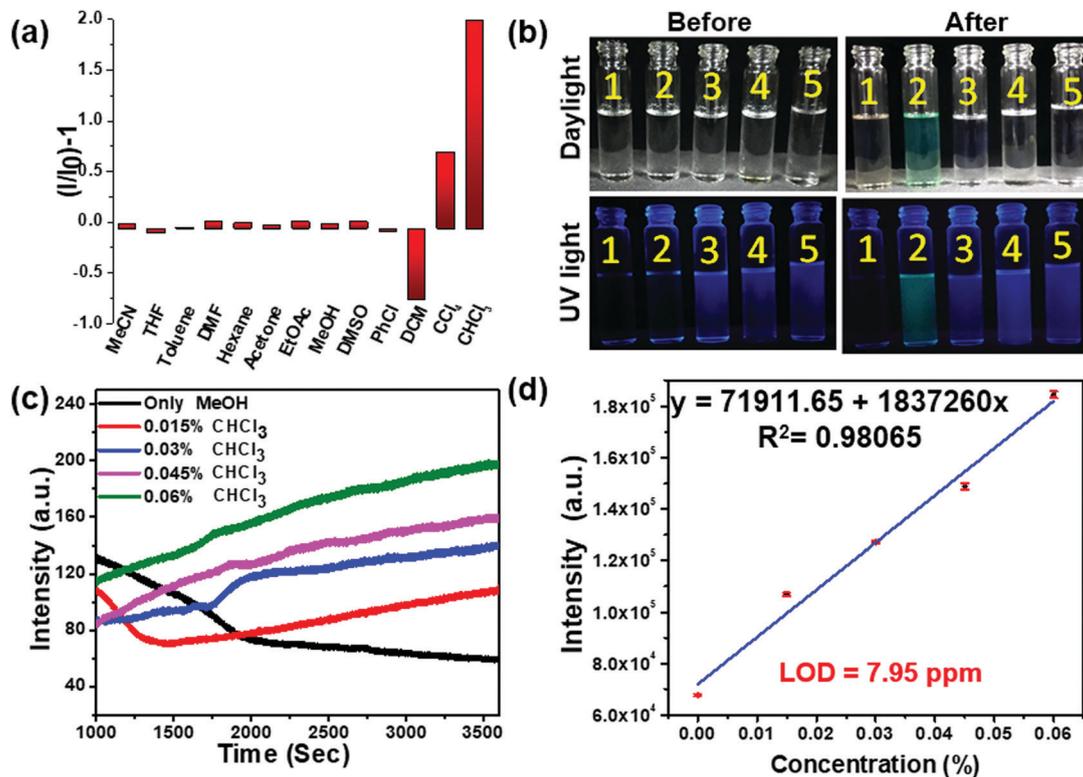

Fig. 3 (a) Selectivity study of the NBMe molecule (20 μM) in the presence of various common organic solvents. (b) Digital photograph of NBMe in different solvents (inset: (1) carbon tetrachloride, (2) chloroform, (3) 1,2-dichloromethane, (4) chlorobenzene, (5) methanol) before and after irradiation for 15 min under 365 nm light. (c) Photo-luminescence kinetics spectra of NBMe (20 μM) with increasing percentage of chloroform recorded up to 1 hour in methanol at room temperature. (d) Fluorescence response of NBMe (20 μM) taken in methanol as a function of chloroform percentage.

(up to ~95%) of the emission intensity was realized in CH_2Cl_2 on exposure to UV light (Fig. 4(c), (d)). Similar to chloroform,

UV/visible studies were conducted for the other three solvents (PhCl, CCl_4, CH_2Cl_2) before and after UV irradiation. The UV/

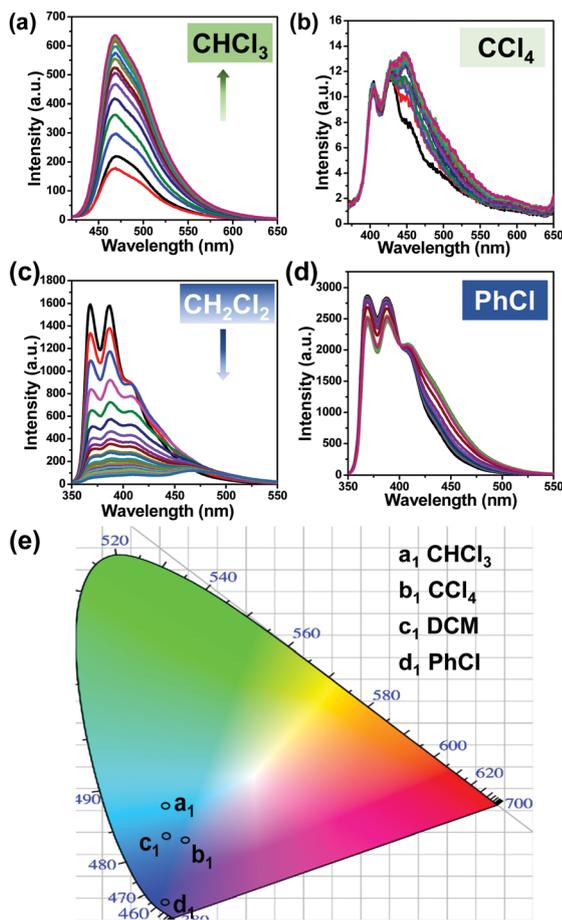© 2022 The Author(s). Published by the Royal Society of Chemistry

Fig. 4 Fluorescence spectra of NBMe (20 μM) in (a) chloroform, (b) carbon tetrachloride, (c) 1,2-dichloromethane, and (d) chlorobenzene with back-to-back reading on excitation at 330 nm. (e) Chromaticity diagram depicting the final emission of the NBMe probe after 15 min 330 nm light excitation in the corresponding solvent.

visible spectra showed no prominent change for PhCl, but a weak band was observed for CH_2Cl_2 and CCl_4 at a longer wavelength (~ 800 nm) without a noticeable decrease in its initial wavelength maxima as compared to that with chloroform (Fig. S4, ESI†). Altogether, the very distinct fluorescence behaviors in the different wavelength windows (Fig. 4(e) and Table S2, ESI†) indicate that these four VCSs could be readily detected and distinguished depending upon the different symmetry and possible interactions between the probe and analyte in the photoinduced ground-state complex of the NBMe probe.

Considering the robust evidence of ground-state complexation from the UV/visible absorption study, we further performed time-resolved PL studies of all the probes in chloroform solution before and after UV irradiation for 15 min using 375 nm pulse excitations (Fig. S5–S8, ESI†). As summarized in Table 1, all the probes displayed single exponential decay corresponding to monomeric emission in the solution. In contrast, dual exponential decay was observed after UV irradiation, indicating the presence of dual components in the solution. The appearance of a long-lived fluorescent component after UV irradiation could be attributed to the formation of a UV radiation-assisted complex between the probe and the chloroform molecule.[26,27]

To further confirm the UV light-assisted complexation of the probes with chloroform along with the site of interaction, time-dependent NMR titration was performed in $CDCl_3$ before and after irradiation under 365 nm UV light (Fig. 5(a)). Importantly, due to the very high sensitivity of the probes towards $CHCl_3$, the titration was carried out with trace $CHCl_3$ present in $CDCl_3$. For the NCPh probe, ^1H NMR studies demonstrated that the aromatic protons lying much closer to the nitrogen atom (c, d, g) expectedly undergo a significant downfield shift compared to the other aromatic protons (e, f). The peak at ~ 4.5 ppm (a) corresponding to the –NH proton disappeared completely on UV irradiation, which was later confirmed by FTIR spectroscopy to be due to the fast solvent proton exchange process (Fig. 5(b)).[28,29] No broadening and shifting of the NH stretching band (~ 3400 cm^{-1}) was observed in the FTIR spectrum, further ruling out the possibility of interaction between NH protons and chloroform molecules.

However, to analyze the radical formation and its role in the photophysical properties, ESR and photoluminescence experiments were carried out in the presence and absence of the radical scavenger (2,2,6,6-tetramethylpiperidin-1-yl)oxyl (TEMPO). The ESR study revealed that only trace amounts of radical generation took place from the probes due to light irradiation (Fig. S9, ESI†). Further, to scrutinize the role of the radicals in the photophysical properties, the fluorescence intensities of all three probes were recorded in the absence and presence of TEMPO in chloroform solution, maintaining a 1:1 and 1:5 ratio of probe to TEMPO (Fig. S10, ESI†). This study revealed that there is no significant change in the emission intensities in all the cases, which also nullified the involvement of radicals in complex formation. Additionally, a temperature-dependent luminescence study was conducted by

Table 1 Summary of the time-resolved PL data of the probe solutions in chloroform before and after UV irradiation for 15 minutes

Name	f_i (%)		τ_i (ns)		Average τ_i (ns)		Chi-square (χ^2)		Exponential fitting	
	Before	After	Before	After	Before	After	Before	After	Before	After
NBMe	100	38.862 61.138	1.681	1.371 5.560	1.681	3.932	1.006	1.013	Mono	Bi
NBPh	100	27.194 72.806	1.692	1.512 5.602	1.692	4.489	1.011	1.008	Mono	Bi
NCPh	100	13.549 86.451	1.596	1.003 6.404	1.596	5.672	1.005	1.006	Mono	Bi

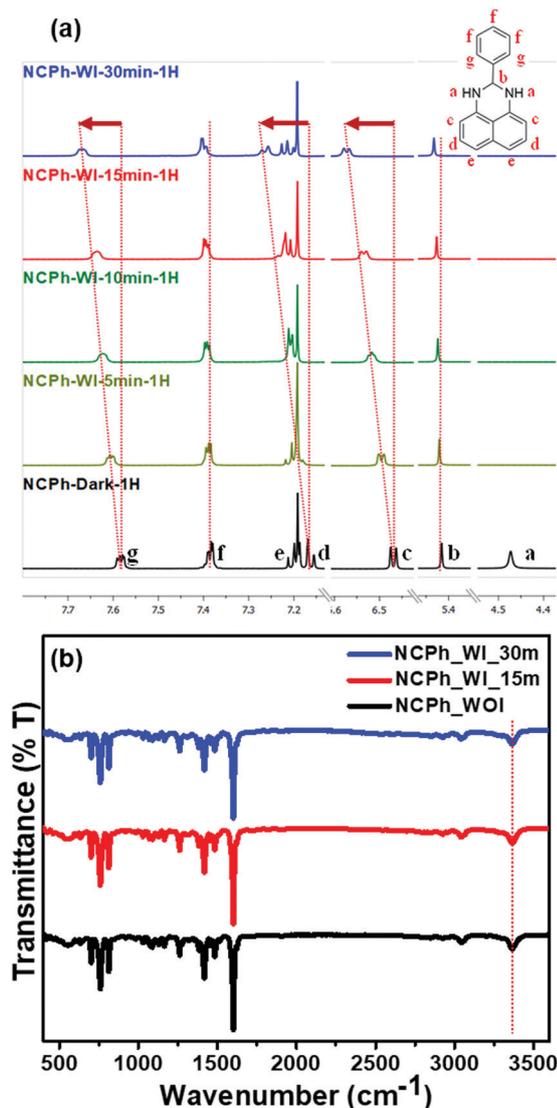Fig. 5 (a) ^{1}H NMR spectra (zoomed) for the titration of NCPh molecules in the presence of deuterated chloroform under dark conditions and on irradiation (WI) with 365 nm UV light with time up to 30 min. (b) FTIR spectra of NCPh molecules in chloroform without irradiation (WOI) and with irradiation (WI).

lowering the temperature from room temperature (25 °C) to −50 °C (Fig. S11, ESI†). All the probes exhibited negligible changes with the lowering of temperature, which suggests that the formation of the photoinduced adduct is not kinetically dependent.

Meanwhile, similar responses for all the three probes in the UV/visible and fluorescence studies confirmed the insignificant role of the boron atom in the complexation process. These results prove that the naphthalene rings play a vital role in the photoinduced ground-state complexation, and indicate the presence of weak π–Cl and CH–π interactions, resulting in the downfield shift of the aromatic protons. Apart from these, other weak Cl–N and CH–N interactions might also trigger the ground-state complexation.[22,30] However, NBMe and NBPh

molecules do not possess much deviation in the ^{1}H NMR signals corresponding to their aromatic cores (Fig. S12 and S13, ESI†). This could be attributed to the formation of a relatively strong interaction between chloroform and the NCPh probe due to its comparatively higher negative potential on the π surface than NBPh and NBMe.

This was further confirmed by the relatively higher color contrast present on the naphthalene ring of the NCPh molecule as visualized in the electrostatic potential diagram (Fig. S14, ESI†).[31–33]

Apart from the light-up colorimetric and fluorometric response of the probes in the solution phase, the sensing responses of the probes towards VCSs vapor were also utilized to develop a portable sensing platform for real-time on-site detection and discrimination (Fig. 6).

The vapor-phase detection of VCSs was performed using cost-effective filter paper-based strips. 10 mM probe solution in methanol was drop-cast on Whatman filter paper with a thin capillary tube in the form of "IITG". After 2 min, when the solvent had evaporated completely at room temperature, the filter paper appeared colorless [Fig. 6(a)(1)]. On exposure to chloroform vapor under 365 nm light, the hidden/colorless encrypted writing of "IITG" lit up in blue-green for NBMe, whereas light green and grey were observed for NBPh and NCPh, respectively [Fig. 6(a)(2) and Movie SV-4–6, ESI†].

This result further justified the formation of photo-assisted ground-state complexation, where the formation of new absorption maxima in the red region was in line with the light-up colorimetric response of the probes (Fig. 2(d)–(f)). However, the negative response on exposure to other solvent vapors demonstrated a highly selective nature towards light-up colorimetric chloroform detection only (Fig. S15, ESI†). Moreover, looking into the practical utility, the visual color change of the filter paper was explored in the presence of chloroform vapor generated from different fractions of chloroform in methanol. It was observed that NBMe was able to display an identifiable color change in the presence of chloroform vapor formed from a 1% chloroform in methanol mixture at room temperature (Fig. S16, ESI†).

Interestingly, in contrast to the NBMe and NBPh probes, the NCPh probe remained non-fluorescent in the solid-state and could not be visualized under UV light, which makes it an ideal candidate for the development of a robust security ink (Fig. 6(b), Fig. S17 and Movie SV-6, ESI†). Since, both UV irradiation and chloroform vapor are simultaneously required to visualize the colorimetric response in NCPh, the developed ink could be termed as a "dual-phase encrypted security ink". "Dual-phase encryption" signifies that the encrypted data (lock) can be decrypted only by exposing the NCPh dip-coated paper strips to both UV light and chloroform vapor (keys) simultaneously. As depicted in Fig. 6(b), the data encrypted with the NCPh ink can only be accessed by exposing it to UV light in the presence of chloroform vapor as dual keys for data decryption. To ascertain the robustness of the NCPh security ink, it was further examined under various common solvent vapors, where none of them were able to decrypt data in the presence of UV irradiation (Fig. S15, ESI†).
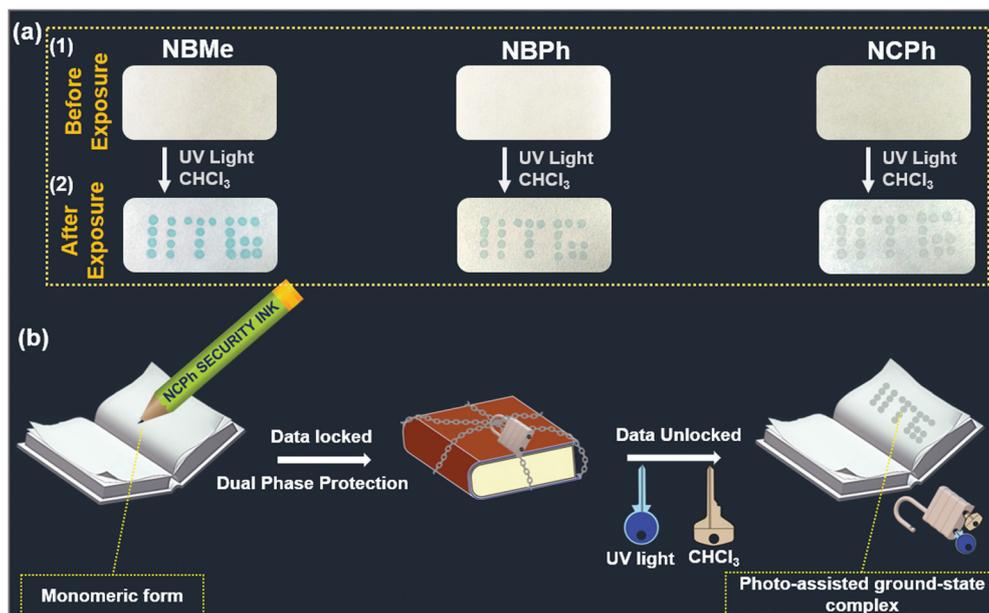
Fig. 6 (a) Picture of the filter paper device fabricated with the probes NBMe, NBPh, and NCPh (1) before and (2) after exposure to chloroform vapor under 365 nm UV light for 2 min, which gave distinct blue–green, light green and grey colors, respectively. (b) Schematic representation of the dual-phase encrypted security ink writing (IITG) being decrypted.

The response of all the naphthalene-based probes towards common VCSs, as found in the digital photographs captured in both the solution and vapor phases (Fig. 3(b) and Fig. S2, S17, ESI†), has been summarized in Fig. 7; the changes in the color signify the changes in the photophysical properties in that particular state.

Considering both the colorimetric and fluorometric responses of the newly developed probes, NBMe could be an ideal probe for the on-site detection and discrimination of VCSs, while NCPh has been established to be an ideal candidate for the development of dual-phase encrypted security ink for data protection (Fig. 7).

Conclusions

In summary, three luminophores have been strategically developed, which can detect chloroform selectively (liquid and vapor) with light-up fluorometric and colorimetric responses *via* UV light-assisted ground-state complex formation with LoD values of 7.95 ppm. Moreover, NBMe could efficiently discriminate different VCSs such as chlorobenzene, 1,2-dichloromethane, carbon tetrachloride, and chloroform as a result of their distinct complexation behavior. Apart from this, the naked eye light-up response on simple filter paper on exposure to UV light in the presence of chloroform vapor provided a cost-effective portable device platform for efficient on-site detection. Further, the solid-state non-fluorescence property of NCPh along with its interaction with chloroform in the presence of UV light has been successfully translated into a robust dual-phase encrypted security ink for locked data protection.

Conflicts of interest

There are no conflicts to declare.

Fig. 7 Summary of the fluorometric and colorimetric responses of the probes towards VCSs. Fluorescence and naked-eye characteristics of the probes in the presence different chlorinated solvents, namely carbon tetrachloride (△), chloroform (◇), 1,2-dichloromethane (●), and chloro-benzene (☆), before and after UV irradiation. ♣, †, and § symbolizes the particular sensing response utilized for the corresponding application.

Acknowledgements

References

1 NR Council, DEL Studies, BCS Technology and CPPLA Update, *Prudent Practices in the Laboratory: Handling and Management of Chemical Hazards, Updated Version*, National Academies Press, 2011.

2 Y. Li, M. E. Calvo and H. Míguez, *Adv. Opt. Mater.*, 2016, **4**, 464–471.

3 L. Vittozzi and E. Testai, *Handbook of Hazardous Materials*, Academic Press, 1993, pp. 119–125.

4 M. Cappelletti, D. Frascari, D. Zannoni and S. Fedi, *Appl. Microbiol. Biotechnol.*, 2012, **96**, 1395–1409.

5 J. K. Wickliffe, T. H. Stock, J. L. Howard, E. Frahm, B. R. Simon-Friedt, K. Montgomery, M. J. Wilson, M. Y. Lichtveld and E. Harville, *Sci. Rep.*, 2020, **10**, 21649.

6 B. Huang, C. Lei, C. Wei and G. Zeng, *Environ. Int.*, 2014, **71**, 118–138.

7 W. T. Tsai, *Rev. Environ. Health*, 2019, **34**, 81–89.

8 R. Gao and D. Yan, *Chem. Commun.*, 2017, **53**, 5408–5411.

9 W. Lindinger and A. Jordan, *Chem. Soc. Rev.*, 1998, **27**, 347–375.

10 R. Lu, W.-W. Li, B. Mizaikoff, A. Katzir, Y. Raichlin, G.-P. Sheng and H.-Q. Yu, *Nat. Protoc.*, 2016, **11**, 377–386.

11 J. L. Martínez-Hurtado, C. A. B. Davidson, J. Blyth and C. R. Lowe, *Langmuir*, 2010, **26**, 15694–15699.

12 A. P. de Silva, H. Q. N. Gunaratne, T. Gunnlaugsson, A. J. M. Huxley, C. P. McCoy, J. T. Rademacher and T. E. Rice, *Chem. Rev.*, 1997, **97**, 1515–1566.

13 X. Z. Lim, *Nature*, 2016, **531**, 26–28.

14 L. Tso-Lun, Lo, S.-W. Lai, S.-M. Yiu and C.-C. Ko, *Chem. Commun.*, 2013, **49**, 2311–2313.

15 Y. Zhou and B. Yan, *Chem. Commun.*, 2016, **52**, 2265–2268.

16 Z.-Z. Lu, R. Zhang, Y.-Z. Li, Z.-J. Guo and H.-G. Zheng, *J. Am. Chem. Soc.*, 2011, **133**, 4172–4174.

17 N. Meher and P. K. Iyer, *Angew. Chem., Int. Ed.*, 2018, **57**, 8488–8492.

18 L. Dai, D. Wu, Q. Qiao, W. Yin, J. Yin and Z. Xu, *Chem. Commun.*, 2016, **52**, 2095–2098.

19 M. Koenig, B. Storti, R. Bizzarri, D. M. Guldi, G. Brancato and G. Bottari, *J. Mater. Chem. C*, 2016, **4**, 3018–3027.

20 L. Ding, Z. Zhang, X. Li and J. Su, *Chem. Commun.*, 2013, **49**, 7319–7321.

21 J. Lee, H. T. Chang, H. An, S. Ahn, J. Shim and J.-M. Kim, *Nat. Commun.*, 2013, **4**, 2461.

22 Q. Wu, H. Ma, K. Ling, N. Gan, Z. Cheng, L. Gu, S. Cai, Z. An, H. Shi and W. Huang, *ACS Appl. Mater. Interfaces*, 2018, **10**, 33730–33736.

23 W.-M. Wan, D. Tian, Y.-N. Jing, X.-Y. Zhang, W. Wu, H. Ren and H.-L. Bao, *Angew. Chem., Int. Ed.*, 2018, **57**, 15510–15516.

24 T. Mori and Y. Inoue, *Chem. Soc. Rev.*, 2013, **42**, 8122–8133.

25 N. Meher, S. Panda, S. Kumar and P. K. Iyer, *Chem. Sci.*, 2018, **9**, 3978–3985.

26 S. Hussain, A. H. Malik and P. K. Iyer, *J. Mater. Chem. B*, 2016, **4**, 4439–4446.

27 C. Biskup, T. Zimmer, L. Kelbauskas, B. Hoffmann, N. Klöcker, W. Becker, A. Bergmann and K. Benndorf, *Microsc. Res. Tech.*, 2007, **70**, 442–451.

28 D. L. Pavia, G. M. Lampman, G. S. Kriz and J. A. Vyvyan, *Introduction to spectroscopy*, Cengage Learning, 2014.

29 B. Ramirez, M. A. Durst, A. Lavie and M. Caffrey, *Sci. Rep.*, 2019, **9**, 12798.

30 S. K. Pandey, *ACS Omega*, 2021, **6**, 11711–11728.

31 P. Politzer, J. S. Murray and T. Clark, *Phys. Chem. Chem. Phys.*, 2010, **12**, 7748–7757.

32 P. C. Rathi, R. F. Ludlow and M. L. Verdonk, *J. Med. Chem.*, 2020, **63**, 8778–8790.

33 R. Garai, R. K. Gupta, A. S. Tanwar, M. Hossain and P. K. Iyer, *Chem. Mater.*, 2021, **33**, 5709–5717.